MultiScience - XXX. microCAD International Multidisciplinary Scientific Conference
University of Miskolc, Hungary, 21-22 April 2016, ISBN 978-963-358-113-1

METHODOLOGY DEVELOPMENT FOR NUMERICAL EVALUATION OF WEAR IN TRIBOLOGICAL CONTACTS

Bergmann Philipp[1], Grün Florian[2], Gódor István[3] and Herbst Klaus[4]
[1, 2, 3]Chair of Mechanical Engineering, Montanuniversität Leoben,
philipp.bergmann@unileoben.ac.at
[4]Miba Gleitlager GmbH, klaus.herbst@miba.com

1. INTRODUCTION

Due to actual legislative regulations for automotive industry implying a cap of average 95 g CO_2/km for an OEM's fleet by 2020 an overall increase of vehicles' efficiency is necessary. Areas which can contribute significantly to this ambitious goal are among others light weight design, downsizing, the reduction of frictional losses and hybridization. Looking onto the topic of hydrodynamic journal bearings in internal combustion engines (ICE) in this context, performed actions lead to higher specific loads and imply hindered conditions. As a consequence the chance of wear and failure increases which needs to be taken into account in a machines design by numerical wear assessments. One of the most prominent wear models goes back to Archard [1]. Based on material parameters and an empirical coefficient this model allows a numerical implementation in the multiphysics simulation software COMSOL [2], [3].

In the following journal bearings' characteristics as well as the impact of actual developments on journal bearings is described with the help of Stribeck-curves. The tribological test methodology developed at the Chair of Mechanical Engineering to calculate necessary wear coefficients of arbitrary material combinations by using a rotationary tribometer TE92HS in combination with a journal bearing adapter (JBA) follows this first part. The setting of the numerical model of the JBA is described and finally numerical and test results are compared.

2. JOURNAL BEARINGS – SETUP AND FUNCTIONALITY

Journal bearings typically comprise of a steel shaft, a softer multilayer journal bearing shell and the lubricant, see figure 1. The relative motion of the shaft and journal bearing results in a fluid film gap geometry allowing a hydrodynamic pressure build up which is in equilibrium with an external load F_{ext}. Dependent on load, rotational speed and temperature the operation point of a journal bearing varies. A Stribeck-curve visualizes this circumstance by plotting the coefficient of friction COF or μ against the Hersey number or in most cases against the relative speed, see figure 2 full line. With increasing Hersey number frictional behaviour changes from solid friction to boundary and mixed friction. During these regimes of friction the surfaces are in contact leading to high frictional losses and wear. After the release point the mating surfaces are separated and the system's behaviour changes to fluid friction in which the conventional area of operation is situated. Increasing shear forces lead to a rise of frictional losses in this regime.

DOI: 10.26649/musci.2016.084

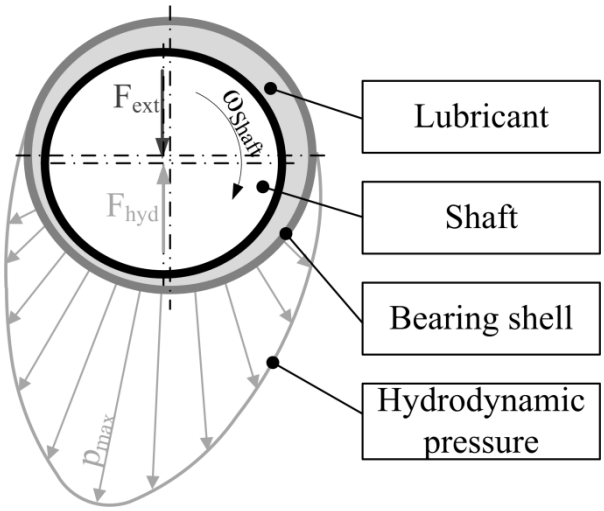

Figure 1: Principle set up of a journal bearing comprising of a shaft, a bearing shell and a lubricant in between separating both surfaces by hydrodynamic pressure.

The intensity of wear is tight-knit to the occurring friction regimes. While solid, boundary and mixed friction regimes generally lead to high wear, wear in fluid friction regime is comparable low [4]. The impact of actual developments including light weight design, downsizing, the reduction of frictional losses and hybridization on the frictional behaviour of journal bearings can be visualized descriptive with help of Stribeck-curves in figure 2. To reduce fluid frictional losses in the conventional area of operation the usage of low and ultra-low viscosity oils is contemplated resulting in lower fluid film thicknesses which widen the area of boundary and mixed friction towards higher rotational speeds [5]. The same line take higher specific loads resulting from downsizing and light weight design. Additionally the upcoming start/stop technology leads to a frequent run through the already widened areas of boundary and mixed friction making wear in journal bearings to a delicate topic [6], [7].

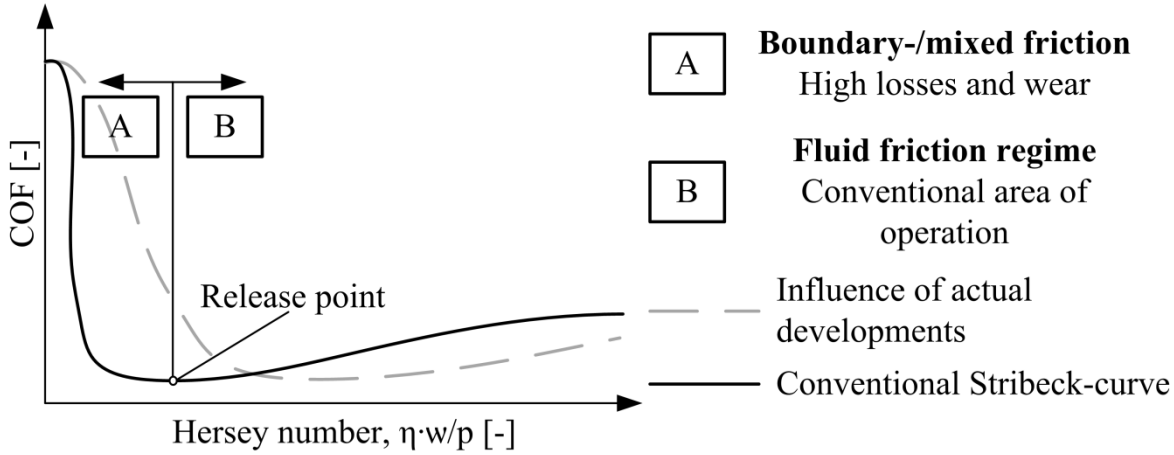

Figure 2: The full line represents a conventional Stribeck-curve. The impact of actual developments is depicted by dashed line.

3. NUMERICAL INCORPORATION OF WEAR LAWS

Wear models link a resulting wear quantity, e.g. wear height or wear volume to the properties of the mating materials and information about the contact state and duration. Archard's law, see equation 1, is widely used and links the worn volume W to the normal force P, the sliding distance s, the flow pressure of the softer material p_m and an empirical material-related constant K, which describes the probability to produce a wear particle [1].

$$W = \frac{K \cdot s \cdot P}{p_m} \tag{1}$$

This wear equation can be incorporated in COMSOL after some mathematic steps by defining an ordinary differential equation (ODE), see equation 2. The material dependent variables K and p_m are combined to the wear intensity C, which describes the dependence of wear volume on frictional energy as a result of solid contact in relative motion. This parameter can be derived from measured test data. By differentiating equation (1) with respect to time and identifying $\partial s/\partial t$ as the sliding velocity v of the counterpart surface and p as the normal pressure acting on the surface, the necessary ODE can be deduced.

$$\frac{\partial w}{\partial t} = C \cdot p \cdot v \tag{2}$$

4. TEST METHODOLOGY

Tests to achieve the necessary wear intensities were conducted on a rotationary tribometer TE92HS from Phoenix Tribology mainly comprising of a motor (I), the shaft (II) and the journal bearing adapter (JBA) (III). The specific set up can be found in [8]. The adapter realizes the tribological system of a real life journal bearing shell and a shaft specimen in an oil bath, which contains the lubricant and can be heated.

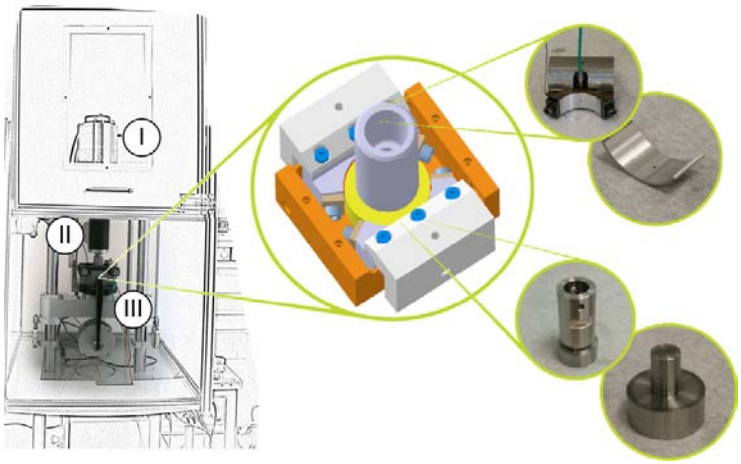

Figure 3: Test set of the rotationary tribometer TE92HS and the journal bearing adapter (JBA).

The input parameters are load p, the system's temperature T_1 and rotational speed n. The system's behaviour can be described using the coefficient of friction (COF), the contact potential (CP) and the close to contact temperature T_2. The CP sheds light on the state of contact, whereby a CP value of 0 mV states direct contact of bearing shell and shaft specimen. A rising CP suggests an increasing separation of the solid surfaces until complete separation of both surfaces by a lubrication film. Additional measurements, in particular the contact close temperature T1 and the hydrodynamic pressure allow more insights of the occurring tribological processes [7]. Figure 4 shows an exemplary graph of a Stribeck-curve and how available measurement data can explain the tribological processes.

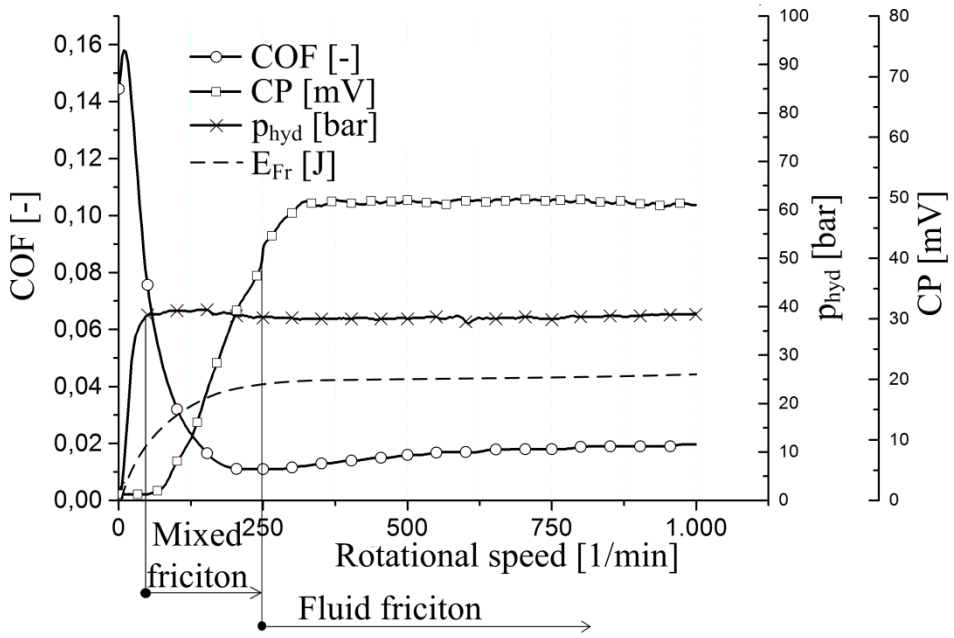

Figure 4: Exemplary Stribeck-curve.

Starting from zero rotational speed the COF sinks with increasing speed. Simultaneously the contact potential as well as the hydrodynamic pressure rise, showing that the load is increasingly carried by the hydrodynamic pressure and the solid contact share reduces. After the release point at around 250 rpm the system operates in fluid friction, indicated by high CP-values and the COF which starts to rise again. Based on the normal force F_N, the measured COF, the rotational speed n, the acquisition frequency f, the shaft specimen radius r and the CP the resulting frictional energy E_{Fr} is calculated. The CP acts as a weighting coefficient to consider the state of friction and the intensity of wear, whereby the CP_{Fluid} indicates the CP value of the fluid friction regime:

$$E_{Fr} = F_N \cdot \mu \cdot \frac{2 \cdot \pi \cdot n \cdot r}{f} \cdot \left(1 - \frac{CP}{CP_{Fluid}}\right) \tag{3}$$

The standard data acquisition mode enables an acquisition frequency of 1 Hz. Since the start/stop cycles occur in a period of time of 5 seconds, this type of data acquisition doesn't deliver enough information. To bypass this lack of information every specified number of cycles the rising ramp is recorded with a frequency of 1

kHz. After an additional cycle the decreasing ramp is also recorded with the same frequency. This in high speed measurement recorded data is taken as representative data for the following cycles. To record wear heights and volume, the thickness of selected points over the specimens' surface as well as the weight of the bearing specimens are measured before and after the tests. The test program of conducted tests is depicted in figure 5.

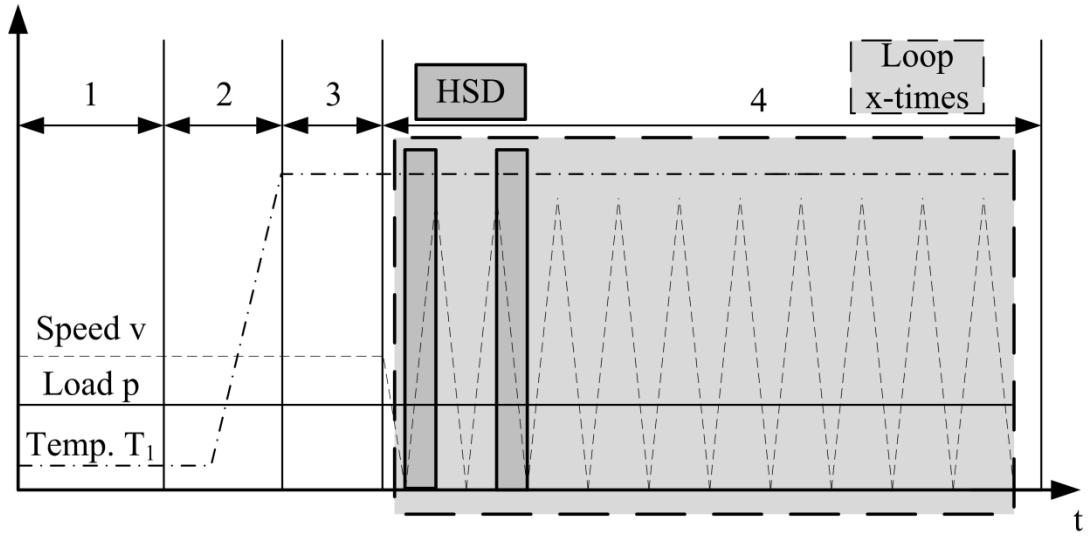

Figure 5: Schematic test program.

After applying the maximum load the system is set to a moderate speed during a running in phase (1). In this step the surfaces adjust to each other leading to an energetic favourable state. In Step 2 the system is heated up to the aspired test temperature. Due to inertial thermal effects a compensation phase (3) is included. The subsequent step 4 includes a defined number of start/stop cycles. By reducing the rotational speed to zero and then starting again while keeping the other parameters constant, the tribological system runs through all regimes of friction. During this time high speed data (HSD) measurements are taken for the calculation of frictional energy. To evaluate the wear intensity tests with varying number of cycles were conducted. The material under investigation was a lead based overlay on a bronze lining and a standard crank shaft steel shaft. Shell Rimula 10W was used as lubricant.

5. TRIBOMETRIC RESULTS

In figure 6 on the left hand side an exemplary test graph showing the run of the contact close temperature T_1, the systems temperature T_2, the COF, and normal load F_N is depicted. Due to the chronological representation the resulting Stribeck-curves reduce to single peaks. Therefore a zoom is shown on the right hand side additionally including the speed and the CP. The system operates in a steady state and wears continuously when low sliding speed leads to an insufficient hydrodynamic pressure build up resulting in solid contact, which is indicated by a breakdown of the CP.

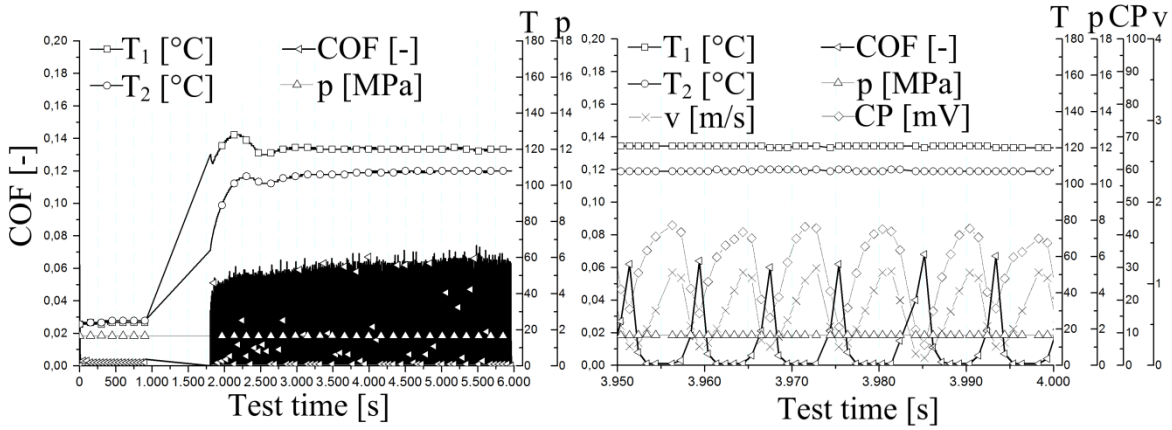

Figure 6: Left: Test plot of a start/stop wear test. Right: Zoomed period of time depicting steady state start/stop behaviour.

With equation (3) the frictional energetic entry can be calculated and plotted in relation to the resulting wear volume, see figure 7. With increasing number of cycles and consequently increasing frictional energy the wear volume increases linearly. This characteristic is comparable to available data in literature and allows retrieving a constant wear intensity C from measured data.

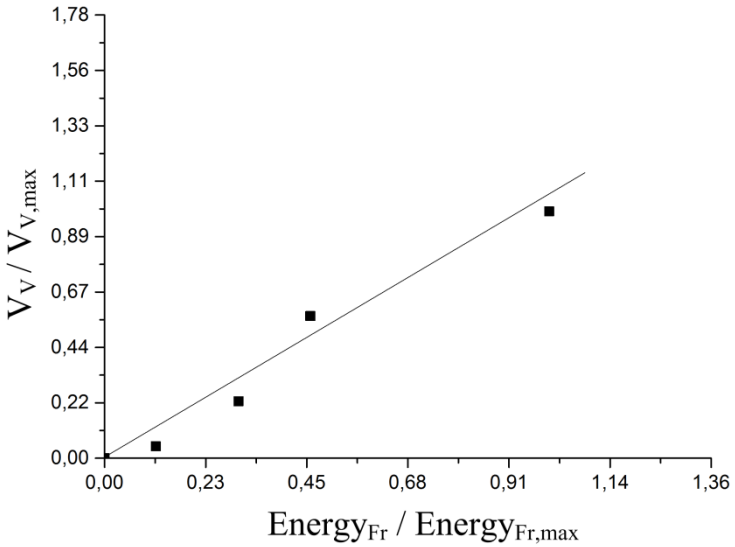

Figure 7: wear characteristic.

6. NUMERICAL MODEL SET UP

A numerical model is set up in COMSOL representing one half of the JBA. The specimen adapter is loaded with a time dependent external force acting on boundary A. On the journal bearing's surface, boundary B, the Reynolds equation is solved so that the external force stays in a dynamic equilibrium with the resulting hydrodynamic pressure. Boundary C, D and E are restrained by roller conditions

only allowing deformation in tangential direction. Additionally the mesh is shown in figure 8, which was chosen rather coarse since the test functions are quadratic and no sharp gradients of the solution are expected.

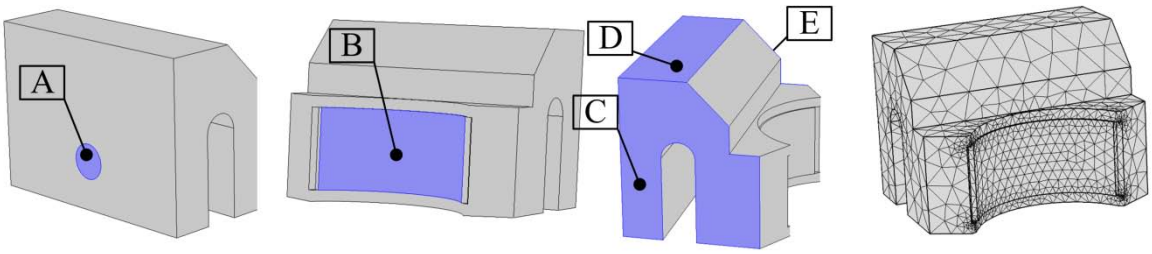

Figure 8: Numerical model set up. Boundary A: external load, boundary B: hydrodynamic load, boundary C, D and E: constraint normal deformation. The mesh is shown on the right hand side.

Deformation of the JBA's structure is taken into account. The shaft specimen, however, can be considered as rigid due to its high stiffness in comparison to the bearing shell and specimen adapter. Subsequently the shaft is not modelled and only considered as shaping geometry of the fluid film. The central axes of the shaft specimen and journal bearing exhibit an angular misalignment which is taken into account in the fluid film geometry. In the case of small film thicknesses surface roughness asperities interact and the surfaces come into contact. To take solid contact into account a contact model according to Greenwood and Williamson was implemented yielding an additional pressure dependent on the fluid film thickness height [9]. This statistical model can be described with equation (4) and can basically be divided in the stiffness part including geometric and material parameter (combined Young's modulus E', asperity density n, mean asperity radius R) of the surface and a standard probability function taking the statistical distribution of the asperity heights into account. d represents the actual fluid film thickness.

$$p = \frac{4}{3} \cdot E' \cdot n \cdot \sqrt{R} \cdot \int_{d}^{\infty} (z-d)^{\frac{3}{2}} \Phi(z) dz \qquad (4)$$

The wear law, equation 2, is implemented by an ODE on the surface of the journal bearing (boundary B). For evaluation purposes of the set up numerical model a period of start/stop was taken into account with parameters taken from the test configuration: FN = 1500 N; n = 0.01 - 500 rpm; T = 110 °C. Since a sliding speed of 0 rpm would lead to a singularity a low rotational speed was chosen to avoid this problem.

7. RESULTS

Figure 9 shows the simulated run of the external load F_{ext}, which is kept constant after ramping it from an initial state, the hydrodynamic load F_{hyd} and the force resulting from solid contact $F_{contact}$. At the initial phase of loading the external force is in equilibrium with the hydrodynamic force only. When the carrying capacity of the hydrodynamic force is exceeded, meaning that the fluid film

thickness drops under the roughness value of the surfaces, the solid contact force contributes to the force equilibrium starting at approximately 40 seconds. Simultaneously process of wear starts and wear volume rises. At 100 seconds start/stop cycles start. As a consequence of the varying rotational speed v (0.01 – 500 rpm) a hydrodynamic carrying capacity changes. The residual load share needs to be carried by solid contact. During the periods of solid contact occurs leading to a resulting cascaded wear volume increase.

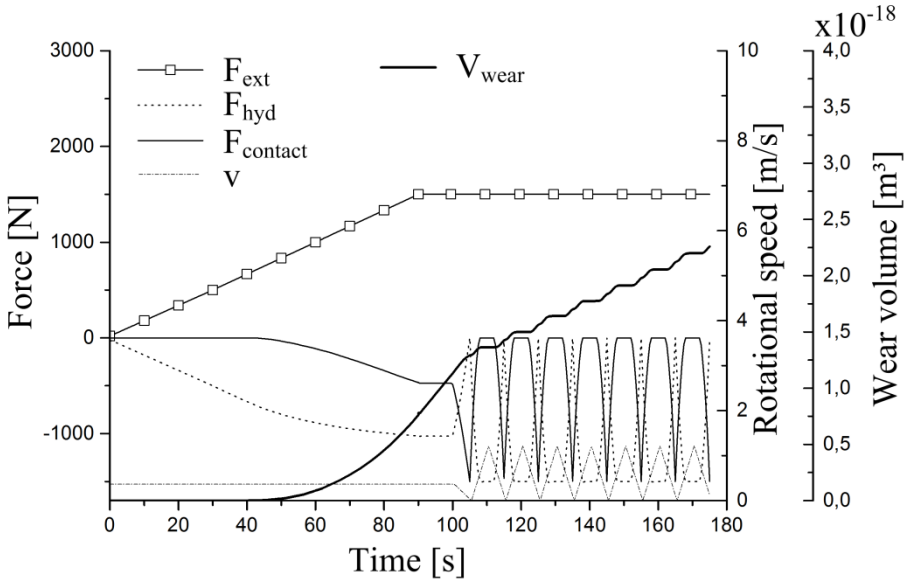

Figure 9: Resulting quantities of the numerical time dependent test sequence.

The simulation was stopped after 7 start/stop cycles. After the performed start/stop cycles an accumulated wear volume 2.27x10-18 m³ and a maximum wear height of µm 2.37E-8 µm arose. The methodology is evaluated by comparing the resulting wear pattern of test (left) and simulation (right), see figure 10. The bearing shell exhibits an area of intense wear at the lower boundary indicated by a darker dislocation. The same holds for the simulated wear pattern.

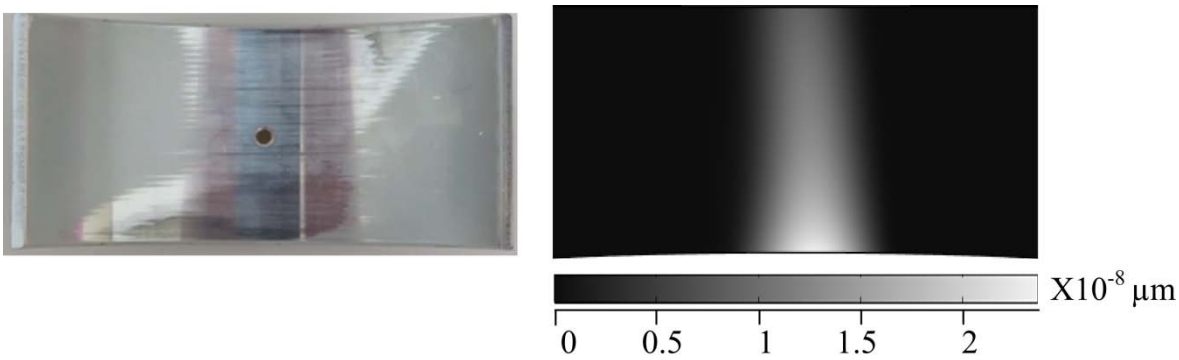

Figure 10: Comparison of contact pattern resulting from numerical investigations (left) and test specimen (right).

8. SUMMARY

- A simulation methodology incorporating a time-dependent wear investigation based on the Archard wear law of the JBA was set up.
- Necessary wear coefficients wear observed by conducting tests on the JBA and consequently a strong relation to the real wear processes in numerical investigations could be incorporated.

9. CONCLUSION

- The developed methodology in COMSOL represents a meaningful and fast to adapt tool to assess wear in arbitrary tribological contacts.
- The reported methodology is capable to consider arbitrary geometry and deviation of the target geometry.

10. ACKNOWLEDGEMENT

Financial support by the Austrian Federal Government (in particular from Bundesministerium für Verkehr, Innovation und Technologie and Bundesministerium für Wissenschaft, Forschung und Wirtschaft) represented by Österreichische Forschungsförderungsgesellschaft mbH and the Styrian and the Tyrolean Provincial Government, represented by Steirische Wirtschaftsförderungs-gesellschaft mbH and Standortagentur Tirol, within the framework of the COMET Funding Programme is gratefully acknowledged. In addition the authors are deeply grateful to the company partner Miba Gleitlager GmbH for their support.

11. REFERENCES

[1] ARCHARD, J. F. and HIRST, W.: **Wear of metals under unlubricated conditions.** Proceedings of the Royal society of London. Series A, Mathematical and Physical Sciences, 1956, pp. 397-410.

[2] ELABBASI, N. H.; HANCOCK, M. J. and BROWN, S. B.: **Simulating Wear in Disc Brakes.** COMSOL Conference 2014, Boston.

[3] SUTTON, D.; LIMBERT, G.; STEWART, D. and WOOD, R. J. K.: **Simulation of Wear using LiveLinkTM for MATLAB®.** COMSOL Conference 2013, Rotterdam.

[4] STACHOWIAK, G. W. and BATCHELOR, A. W.: **Engineering Tribology**, 3rd Edition, Elsevier Butterworth-Heinemann, 2005, ISBN-13:978-0-7506-7836-0.

[5] MARTINEZ, B. T.; MARTINEZ, V. M.; ROA, L. R. and GUTIÉRREZ, T. P.: **Evaluation of the Fuel Economy Improvement due to Low Viscosity Lubricants in a Light Duty Diesel Engine Running under the New European**

Driving Cycle (NEDC). 19th International Colloquium Tribology - Industrial and Automotive Lubrication, 2014, Stuttgart, Germany.

[6] SUMMER, F.: **Tribometric assessment towards functionality of current and future journal bearing systems.** Montanuniversität Leoben, Phd-thesis, 2016.

[7] BERGMANN, P.; SUMMER, F.; GRÜN, F.; GÓDOR, I.; OFFENBECHER, M. and LAINÉ, E.: **Tribological Investigations of Journal Bearings by means of a close to component Test Methodology**. ÖTG Symposium 2014, pp. 113-121.

[8] GRÜN, F.; KRAMPL, H.; SCHIFFER, J.; MODER, J.; GÓDOR, I. and OFFENBECHER, M.: **Tribometric Development Tools for Journal Bearings – a novel test adapter.** World Tribology Congress 2013.

[9] GREENWOOD, J. A. and WILLIAMSON, J.B.P.: **Contact of Nominally Flat Surfaces.** Proceedings of the Royal society of London. Series A, Mathematical and Physical Sciences, 1966, pp. 300-319.